

A Minimal Set of Coordinates for Describing Humanoid Shoulder Motion

David Ingram¹, Christoph Engelhardt², Alain Farron³, Alexandre Terrier² and Philippe Müllhaupt¹

Abstract—The kinematics of the anatomical shoulder are analysed and modelled as a parallel mechanism similar to a Stewart platform. A new method is proposed to describe the shoulder kinematics with minimal coordinates and solve the indeterminacy. The minimal coordinates are defined from bony landmarks and the scapulothoracic kinematic constraints. Independent from one another, they uniquely characterise the shoulder motion. A humanoid mechanism is then proposed with identical kinematic properties. It is then shown how minimal coordinates can be obtained for this mechanism and how the coordinates simplify both the motion-planning task and trajectory-tracking control. Lastly, the coordinates are also shown to have an application in the field of biomechanics where they can be used to model the scapulohumeral rhythm.

Index Terms—shoulder kinematics, joint coordinates, minimal coordinates, motion planning.

I. INTRODUCTION

The shoulder is a complex part of the human body. Comprised of three bones, three joints, and the thorax, it is capable of performing sophisticated motions due to a kinematically redundant structure. To achieve the level of performance, humans solve the indeterminacy using a highly evolved coordination strategy known as the scapulohumeral rhythm. These attributes make the shoulder a very attractive system to mimic.

Over the years, numerous models of the system have been developed by the biomechanics community to try to reproduce the mobility and coordination of the system. The first shoulder model used linkages to describe the movement of the bones [1]. A later model was developed, where each joint was modelled using ideal mechanical joints (spherical, universal) and joint coordinates were introduced [2], [3]. The maximal range of motion of each joint was modelled using joint sinus cones constructed from measured data [4], [5]. A similar model was used to develop a non-linear regression model of the scapulohumeral rhythm (coordinated motion patterns of scapula and humerus), where the joint coordinates of the scapula and clavicle are expressed as non-linear functions of the humeral joint coordinates [6], [7]. The last model representing a significant contribution was developed by van der Helm [8], where the contact between the scapula and thorax was modelled by imposing that the

scapula remain in contact with the surface of an ellipsoid representing the thorax.

Since the van der Helm model was developed, there has been little change in modelling techniques, and his model remains a benchmark. In 2005, the international society of biomechanics (ISB) standardised the modelling process by defining a specific set of coordinates and reference systems for describing the geometry and kinematics [9].

Because of the technological difficulties involved in mimicking human joints and motion, it is only in recent years that mechanisms have been developed with similar kinematic properties as the shoulder. In [10] a mechanical shoulder is proposed based on the observations from Leonardo da Vinci's *Vetruvian Man*. In [11] and [12] parallel architectures are proposed. In [13] a spherical architecture is proposed to replicate the range of motion. In [14] a humanoid shoulder is proposed incorporating a shoulder blade and in [15] the scapulothoracic contact is mimicked.

Thus, the shoulder has been extensively modelled for biomechanics purposes and we are rapidly improving our ability to mimic its behaviour mechanically. However, reproducing the level of coordination exhibited by scapulohumeral rhythm remains a difficult problem because it is not easily measured. In biomechanics, the main solution is to use regression models [7], [16], [17]. In robotics, inverse kinematics is the most widely used approach [12], [18]. Regression models are biomechanically accurate but are mainly linear models and can only replicate the coordination locally. Inverse kinematics solutions are difficult to apply because the coordination is difficult to formulate mathematically due to its nonlinearity.

The goal of this paper is therefore to present a kinematic model of the anatomical shoulder as defined by the biomechanics community, and to propose a new method of solving its kinematic redundancy. To this affect, minimal coordinates are constructed from a geometric description of the shoulder model. Independent from one another, they uniquely describe any motion of the shoulder. Through the kinematic analysis, the shoulder is shown to be a parallel mechanism and a discussion is presented on the possibility of developing a humanoid mechanism with identical kinematic characteristics. The minimal coordinates are shown to be particularly well suited for the motion planning and control of such a mechanism. Lastly, a biomechanics application for modelling the scapulohumeral rhythm is discussed.

¹D. Ingram and Ph. Müllhaupt are with Faculty of Mechanical Engineering, Laboratoire d'Automatique, Ecole Polytechnique Fédérale de Lausanne, 1015 Lausanne, Switzerland.

²Ch. Engelhardt and A. Terrier are with Faculty of Mechanical Engineering, Laboratory of Biomechanical Orthopedics, Ecole Polytechnique Fédérale de Lausanne, 1015 Lausanne, Switzerland.

³A. Farron is with University Hospital Center and University of Lausanne, 1015 Lausanne, Switzerland.

II. KINEMATICS OF THE SHOULDER

A. Skeletal Structure

The skeletal structure of the shoulder is comprised of three bones: the clavicle (c), scapula (s) and humerus (h). The bones are connected together by two joints. The acromioclavicular joint (AC) connecting the clavicle to the scapula and the glenohumeral joint (GH) connecting the scapula to the humerus. A third joint, the sternoclavicular joint (SC), connects the clavicle to the sternum, thereby linking the shoulder to the thorax (Fig. 1).

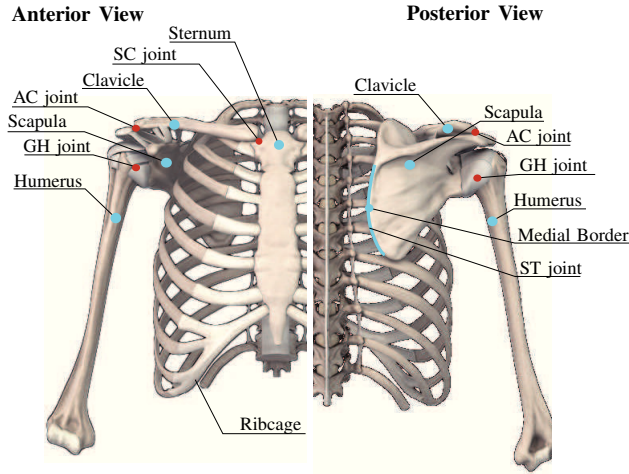


Fig. 1. Illustration of the shoulder skeletal structure.

A second connection exists between the shoulder bones and thorax, known as the scapulothoracic gliding plane (ST). The underside of the scapula's medial border glides over the surface of the ribcage. The scapulothoracic joint is not a joint in the anatomical sense because it does not have ligaments or capsules holding the bones together. Contact is held by the action of a number of muscles, which keep the scapula pressed against the thorax, making the scapulothoracic gliding plane a joint in the kinematic sense. The importance of this joint is two-fold. Kinematically, the contact constrains the system motions, while dynamically the contact surface absorbs part of the load [8].

B. Bony Landmarks & Geometric Model

The skeletal structure is reduced, in terms of geometry, to a set bony landmarks. There are six landmarks necessary to describe the geometry of the shoulder with respect to an absolute reference point (Fig. 2):

- 1) IJ : Jugular Incision & Absolute reference point,
- 2) SC : Center of Sternoclavicular joint,
- 3) AC : Center of Acromioclavicular joint,
- 4) GH : Center of Glenohumeral joint,
- 5) HU : Center of Humeroulnar joint,
- 6) TS : Trigonum Spinae (superior point on medial border),
- 7) AI : Angulus Inferior (inferior point on medial border),

The geometric model is constructed by reducing each bone to a subset of bony landmarks, yielding a characteristic length

or shape. The clavicle is represented by the line segment between the SC and AC joints. The scapula is characterised by the quadrilateral formed by the AC joint, the GH joint and the two end points of the scapula's medial border (TS & AI). The humerus is characterised by the line segment from the GH joint to the humeroulnar joint centre (HU).

C. Kinematic Model

The shoulder is comprised of three moving parts: the clavicle, scapula and humerus, which rotate around the different joints. The thorax (sternum & ribcage) constitutes the frame and reference point for the motion.

The system has three physiological joints (SC, AC & GH) and one purely kinematic joint (ST). The three joints are modelled as spherical joints, while the scapulothoracic joint is modelled using two spherical slider joints (Fig. 3). The two points at either end of the scapula's medial border are constrained to glide over a surface approximating the ribcage, similar to the models from [8], [19], [20].

The system has 7 degrees of freedom according to the following formula

$$M = 6n - \sum_{j=1}^m (6 - k_j) = 7, \quad (1)$$

where $n = 3$ is the number of links, $m = 5$ is the number of joints and k is the associated degrees of freedom (DOF) (Fig. 3).

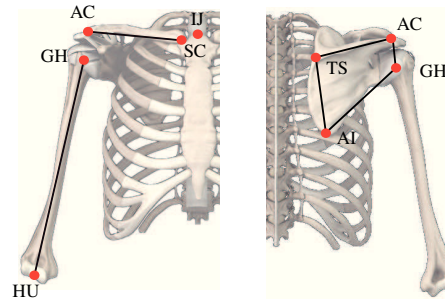


Fig. 2. Bony landmarks and characteristic geometry of the shoulder bones.

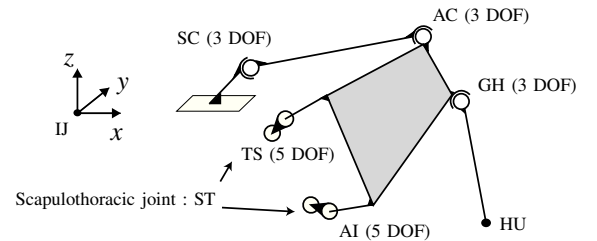


Fig. 3. Kinematic diagram of the shoulder skeletal structure.

D. Reference Frames & Joint Coordinates

Since bones rotate around joints, joint rotation coordinates are a natural choice. Consequently, each bone is attributed with a reference system $(\mathbf{e}_1^i \mathbf{e}_2^i \mathbf{e}_3^i, i = c, s, h)^1$, placed at the

¹Notation: bold lower-case letters are vectors, bold upper-case letters are matrices, plain lower-case letters are scalars and plain upper-case letters are geometric points.

centre of the joint around which it rotates (Fig. 4). The humerus rotates around the GH joint, the scapula rotates around the AC joint and the clavicle rotates around the SC joint. The orientation of each reference frame is defined according to the recommendations set by the International Society of Biomechanics (ISB) [9].

The joint coordinates are defined as Euler angles. The 2-1-3 sequence is used to define the rotations of the clavicle and scapula around the SC and AC joints respectively. The 2-1-2 sequence is used to describe the rotation of the humerus around the GH joint. Thus, each joint is attributed a set of three coordinates

$$\mathbf{x}_c = (\theta_2^c \theta_1^c \theta_3^c)^T, \quad \mathbf{x}_s = (\theta_2^s \theta_1^s \theta_3^s)^T, \quad \mathbf{x}_h = (\theta_2^h \theta_1^h \theta_3^h)^T. \quad (2)$$

The joint angles are referenced by defining the zero rotation configuration of a joint, when its reference system is aligned with the absolute reference system.

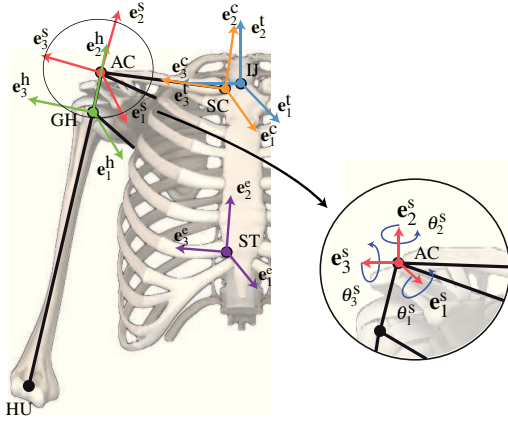


Fig. 4. Joint Reference Systems and Coordinates associated to each joint.

Consider \mathbf{p}_j ($j = c, s, h$), a point on a bone, defined in the local reference system. The position of the same point in the absolute reference system is defined by

$$\mathbf{q}_c = \mathbf{R}_c \mathbf{p}_c + \mathbf{SC}_t, \quad (3)$$

$$\mathbf{q}_s = \mathbf{R}_s \mathbf{p}_s + \mathbf{AC}_t = \mathbf{R}_s \mathbf{p}_s + \mathbf{R}_c \mathbf{AC}_c + \mathbf{SC}_t, \quad (4)$$

$$\mathbf{q}_h = \mathbf{R}_h \mathbf{p}_h + \mathbf{GH}_t = \mathbf{R}_h \mathbf{p}_h + \mathbf{R}_s \mathbf{GH}_s + \mathbf{R}_c \mathbf{AC}_c + \mathbf{SC}_t. \quad (5)$$

The subindexes on the points indicate the reference system where the point is defined. The local to absolute reference frame rotation matrices \mathbf{R}_j are defined as

$$\mathbf{R}_j = \mathbf{R}_j(\mathbf{x}_j) = \mathbf{R}(\theta_2^j) \mathbf{R}^T(\theta_1^j) \mathbf{R}(\theta_3^j), \quad j = c, s, \quad (6)$$

$$\mathbf{R}_h = \mathbf{R}_h(\mathbf{x}_h) = \mathbf{R}(\theta_2^h) \mathbf{R}^T(\theta_1^h) \mathbf{R}(\theta_3^h), \quad (7)$$

$$\mathbf{R}(\theta_1^j) = \begin{bmatrix} 1 & 0 & 0 \\ 0 & c_j & -s_j \\ 0 & s_j & c_j \end{bmatrix}, \quad \mathbf{R}(\theta_2^j) = \begin{bmatrix} c_j & 0 & -s_j \\ 0 & 1 & 0 \\ s_j & 0 & c_j \end{bmatrix}, \quad \mathbf{R}(\theta_3^j) = \begin{bmatrix} c_j & -s_j & 0 \\ s_j & c_j & 0 \\ 0 & 0 & 1 \end{bmatrix},$$

with $c \equiv \cos(\theta)$, $s \equiv \sin(\theta)$.

E. Scapulothoracic Gliding Plane

The ST joint is modelled using two spherical slider joints. The two end-points of the scapula's medial border are constrained to remain in contact with the ribcage, approximated as an ellipsoid using CT scans (Fig. 5), which best fits the

area over which the scapula glides [8], [20]. To account for the layer of muscle tissue between the scapula and ribcage, the points TS and AI are then projected onto the ellipsoid along the normal to the surface, yielding two new points TSp and AIp. The joint model is defined by constraining the distances between the points TS and AI and their projection to remain constant, leading to two holonomic constraints, polynomial functions of the SC and AC joint coordinates. A detailed construction of the constraints is given in the appendix A.

$$\Phi_{TS}(\mathbf{x}_c, \mathbf{x}_s) = 0, \quad \Phi_{AI}(\mathbf{x}_c, \mathbf{x}_s) = 0. \quad (8)$$

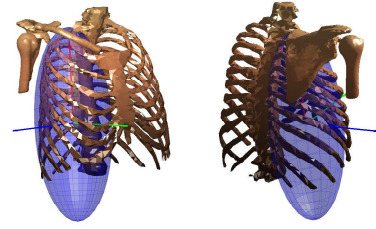


Fig. 5. Representation of the original thorax ellipsoid defining the scapulothoracic joint.

F. Forward Kinematic Model

The forward kinematic shoulder model is defined by choosing the point HU as the end-effector and imposing the scapulothoracic gliding plane constraints on the map (5).

$$\zeta_S : \mathcal{X}_S \rightarrow \mathcal{W}_S \subset \mathbb{R}^3,$$

$$\mathbf{x} = (\mathbf{x}_c, \mathbf{x}_s, \mathbf{x}_h) \mapsto \zeta_S(\mathbf{x}) = \mathbf{R}_h \mathbf{HU}_h + \mathbf{R}_s \mathbf{GH}_s + \mathbf{R}_c \mathbf{AC}_c + \mathbf{SC}_t, \quad (9)$$

$$\text{s.t. } \Phi_{TS}(\mathbf{x}_c, \mathbf{x}_s) = 0, \quad \text{TS contact constraint}, \quad (10)$$

$$\Phi_{AI}(\mathbf{x}_c, \mathbf{x}_s) = 0, \quad \text{AI contact constraint}, \quad (11)$$

The spaces \mathcal{X}_S and \mathcal{W}_S are the joint space and end-effector work space respectively [21].

Defined by 9 coordinates subject to two equality constraints, the joint space \mathcal{X}_S is an embedded sub-manifold of dimension 7. The range space \mathcal{W}_S of ζ_S is a subset of \mathbb{R}^3 analyzed in [4], [22], [23]. The humerus and clavicle rotate around their longitudinal axes without changing the end-effector position, the shoulder is therefore a redundant system of degree 2 [24].

G. The Scapulohumeral Rhythm

The scapulohumeral rhythm defines the coordinated motion of the scapula relative to the humerus. As the humerus moves, the scapula is observed to move in similar fashion but with less amplitude. To illustrate this point, consider raising the arm in the scapular plane (plane parallel to the triangular shape of the scapula). As the humerus rotates upwards or abducts, the scapula rotates by a fraction of the angle. When measured the scapulohumeral rhythm can differ significantly from one individual to another and is of a highly nonlinear nature. The observations from [25] indicate a ratio of 1/3

between the absolute angles (Fig. 6), but this description is not universal and others have been proposed [26], [27], [17], leaving a certain freedom in modelling the shoulder rhythm.

The coordinated motion of the shoulder is achieved through control of the surrounding muscles. The scapulohumeral rhythm is therefore not naturally associated with the kinematic model, but rather represents nature's solution to the kinematic redundancy of the shoulder.

Modeling the scapulohumeral rhythm is not without difficulty since there is no exact definition as stated previously. The main approach thus far has been to use regression models constructed from measured data [7], [16], [17]. This yields a set of functions describing the AC and SC joint angles in terms of the glenohumeral joint angles. The models are mostly linear and therefore model the rhythm locally [16], [17].

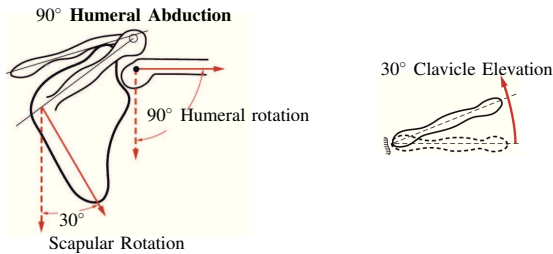


Fig. 6. Schematic description of scapulohumeral rhythm presented in [25].

III. MINIMAL COORDINATES

A. The Shoulder as a Parallel Mechanism

The parallel nature of the shoulder is not directly obvious from the structure of the model previously described. Further analysis of the system shows the shoulder to be comprised of a series mechanism: the humerus, and a closed-loop parallel mechanism: the shoulder girdle. Defined by the thorax, clavicle and scapula, the shoulder girdle forms a parallel mechanism similar to a 3-3 Stewart-Gough platform (Fig. 7). The 3-3 or 3-SPS Stewart platform is defined as a platform supported by ball joints over three legs of adjustable lengths connected to the base through ball joints [28]. In contrast the shoulder girdle is defined as a platform (scapula) supported by three ball joints (AC, TS & AI) over three legs. The first leg (clavicle) is of fixed length and connected to the base (thorax) through a ball joint (SC). The other two legs are of adjustable lengths and are connected to the base through two superimposed universal joints (ST). The lengths of the adjustable legs are constrained and depend on the orientations of the legs with respect to the base. This constraint imposes the scapulothoracic gliding plane.

The purpose of the parallel structure is to increase the range of the glenohumeral joint. The shoulder girdle acts as a positioning and orienting mechanism for the glenohumeral joint, thereby increasing its range. The entire shoulder structure thus represents a highly efficient parallel manipulator.

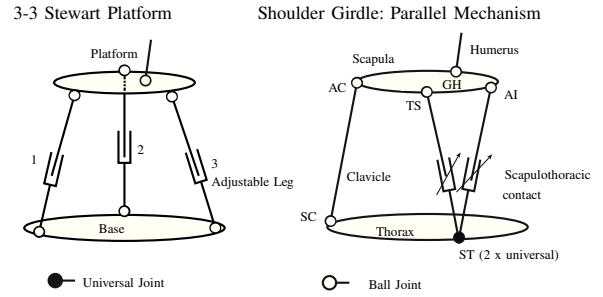


Fig. 7. Diagrams of the 3-3 Stewart platform and shoulder girdle.

B. Minimal Coordinates

The following discussion considers the shoulder mechanism as presented in Figure 8. A platform supported by three links, two of which are of adjustable lengths. On the platform sits a fourth link. The kinematics of this model are defined by the same forward kinematic map (9) subject to the same constraints (10)-(11). To solve the kinematic redundancy a minimal set of 7 independent coordinates are proposed which, provide a simple manner of describing the system's motion.

$$\mathbf{m} = (m_1 \ m_2 \ m_3 \ m_4 \ m_5 \ m_6 \ m_7)^T. \quad (12)$$

The 7 degrees of freedom are defined as follows: 5 degrees of freedom (m_2 to m_6) define the position of the end-effector E (Fig. 8) and 2 degrees of freedom (m_1 & m_7) define the self rotations of the links $B_1 - P_1$ and $P_4 - E$.

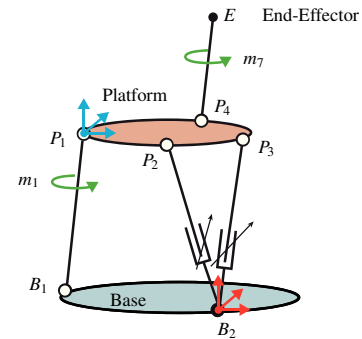


Fig. 8. Diagram of the shoulder parallel mechanism.

The 5 coordinates are defined using a geometric description of the model. The absolute origin is placed at the centre of the superimposed universal joints B_2 and cartesian coordinates are attributed to each point (18 coordinates total).

$$\mathbf{B}_1 = \begin{pmatrix} x_1 \\ x_2 \\ x_3 \end{pmatrix}, \quad \mathbf{P}_1 = \begin{pmatrix} y_1 \\ y_2 \\ y_3 \end{pmatrix}, \quad \mathbf{P}_2 = \begin{pmatrix} z_1 \\ z_2 \\ z_3 \end{pmatrix}, \quad (13)$$

$$\mathbf{P}_3 = \begin{pmatrix} u_1 \\ u_2 \\ u_3 \end{pmatrix}, \quad \mathbf{P}_4 = \begin{pmatrix} v_1 \\ v_2 \\ v_3 \end{pmatrix}, \quad \mathbf{E} = \begin{pmatrix} w_1 \\ w_2 \\ w_3 \end{pmatrix}. \quad (14)$$

The spatial configuration of the points with respect to each other and to the origin is defined by a set of 8 polynomial

equations.

$$(y_1 - x_1)^2 + (y_2 - x_2)^2 + (y_3 - x_3)^2 = \|\mathbf{P}_1 - \mathbf{B}_1\|_2^2, \quad (15)$$

$$(z_1 - y_1)^2 + (z_2 - y_2)^2 + (z_3 - y_3)^2 = \|\mathbf{P}_2 - \mathbf{P}_1\|_2^2, \quad (16)$$

$$(u_1 - y_1)^2 + (u_2 - y_2)^2 + (u_3 - y_3)^2 = \|\mathbf{P}_3 - \mathbf{P}_1\|_2^2, \quad (17)$$

$$(v_1 - y_1)^2 + (v_2 - y_2)^2 + (v_3 - y_3)^2 = \|\mathbf{P}_4 - \mathbf{P}_1\|_2^2, \quad (18)$$

$$(z_1 - u_1)^2 + (z_2 - u_2)^2 + (z_3 - u_3)^2 = \|\mathbf{P}_2 - \mathbf{P}_3\|_2^2, \quad (19)$$

$$(z_1 - v_1)^2 + (z_2 - v_2)^2 + (z_3 - v_3)^2 = \|\mathbf{P}_2 - \mathbf{P}_4\|_2^2, \quad (20)$$

$$(u_1 - v_1)^2 + (u_2 - v_2)^2 + (u_3 - v_3)^2 = \|\mathbf{P}_3 - \mathbf{P}_4\|_2^2, \quad (21)$$

$$(w_1 - v_1)^2 + (w_2 - v_2)^2 + (w_3 - v_3)^2 = \|\mathbf{E} - \mathbf{P}_4\|_2^2, \quad (22)$$

where $\|\cdot\|_2$ is the Euclidean norm. The two constraint equations (10)-(11) are added, yielding a set of 10 equations.

$$\mathbf{P}_2 : \frac{z_1^2}{a^2} + \frac{z_2^2}{b^2} + \frac{z_3^2}{c^2} - 1 = 0, \quad (23)$$

$$\mathbf{P}_3 : \frac{u_1^2}{a^2} + \frac{u_2^2}{b^2} + \frac{u_3^2}{c^2} - 1 = 0, \quad a, b, c : \text{ellipsoid axes lengths.} \quad (24)$$

The point SC is fixed with respect to the origin. Therefore, the 10 equations are function of 15 cartesian coordinates, which can be reduced to 5.

To begin the coordinate reduction, the point E is defined by the sphere equation (22), and can be parameterized using two spherical coordinates α and β .

$$\mathbf{E} : \begin{cases} \|\mathbf{E} - \mathbf{P}_4\| \cos(\alpha) \sin(\beta) + v_1, \\ \|\mathbf{E} - \mathbf{P}_4\| \sin(\alpha) \sin(\beta) + v_2, \\ \|\mathbf{E} - \mathbf{P}_4\| \cos(\beta) + v_3. \end{cases} \quad (25)$$

The position of the point P_4 is defined with respect to the platform origin located at P_1 . To define the configuration (position & orientation) of the platform, the position of three points are needed. To start, the point P_3 is defined by the ellipsoid equation (24). Its motion can be described using the spherical coordinates γ and ν .

$$\mathbf{P}_3 : \begin{cases} a \cos(\gamma) \sin(\nu), \\ b \sin(\gamma) \sin(\nu), \\ c \cos(\nu). \end{cases} \quad (26)$$

The point P_2 lies on the intersection of the sphere defined by (19) and the ellipsoid defined by (23). The intersection defines a locus of points homeomorphic to a circle, which depends on the position of the point P_3 . Practically, the locus is defined by expressing two of the three coordinates of the point P_2 in terms of the third and the coordinates of the point P_3 . The explicit computation of the locus is given in appendix B.

$$\mathbf{P}_2 : \begin{cases} z_1(z_3, u_1, u_2, u_3) = z_1(z_3, \gamma, \nu), \\ z_2(z_3, u_1, u_2, u_3) = z_2(z_3, \gamma, \nu), \\ z_3. \end{cases} \quad (27)$$

Once the locations of P_2 and P_3 are known, the point P_1 is located at the intersection of three spheres centred on B_1 , P_2 and P_3 ((15)-(17)). The resulting locus of the intersection is a pair of points, one of which is the desired point.

The definition of the points P_1 , P_2 and P_3 completely defines the configuration of the platform and therefore the

mechanism. The 5 coordinates necessary to describe the configuration of the six points B_1 , P_1 , P_2 , P_3 , P_4 and E are

$$(\gamma, \nu, z_3, \alpha, \beta). \quad (28)$$

The two remaining coordinates, defining the self rotations of the links $B_1 - P_1$ and $P_4 - E$, do not change the configuration of the six points. However, since these links correspond to the clavicle and humerus which are 3D solids, these rotations are necessary to fully define the configuration of the shoulder skeletal structure. Lastly, the spherical coordinates α and β of the humeral motion are equivalent to the two Euler angles from the joint coordinate model ((9)-(11)): $\theta_1^h = \alpha$, $\theta_2^h = \beta$. The 7 minimal coordinates are given by

$$\mathbf{m} = (\theta_1^c, \gamma, \nu, z_3, \theta_1^h, \theta_2^h, \tilde{\theta}_2^h)^T. \quad (29)$$

C. Mapping Minimal Coordinates to Joint Coordinates

The proposed minimal coordinates solve the motion planning problem efficiently but constructing a dynamic model is not straightforward. Therefore, it is necessary to construct a map between them and the joint angles which are suitable for dynamic modelling.

$$\chi : \mathcal{M}_S \subset \mathbb{R}^7 \rightarrow \mathcal{X}_S \subset \mathbb{R}^9, \\ \mathbf{m} \mapsto \chi(\mathbf{m}) = \mathbf{x}. \quad (30)$$

The map is constructed by computing the local reference-frame vectors of each bone in terms of the minimal coordinates. The rotation matrix to pass from the absolute reference frame is then defined and the joint angles are extracted knowing that the sequence is 2-1-3, as stated previously in Section II-D. This method is possible since the initial configuration of each reference frame is known through the geometric dataset.

D. Remarks

The polynomial description of the system illustrates a number of differences between the shoulder and Stewart platform. Both systems can be described using polynomial equations and share 8 out of 10 of the equations. However, the Stewart platform has legs of variable length, and therefore certain terms on the righthand side are not constant. Also the last two equations ((23)-(24)) differ. A more in-depth comparison between the two mechanisms could be achieved using reduction theory and Groebner basis on polynomial ideals [29], [30]. The minimal coordinates also provide a means of analysing the topological structure of the configuration manifold \mathcal{M}_S . This in turn could lead to a better understanding of the scapulohumeral rhythm.

IV. DISCUSSION

A. Humanoid Mechanism Design

The comparison of the shoulder skeletal structure to the Stewart platform leads to the natural question of whether a mechanical system can be constructed with identical or similar kinematic characteristics to that of the shoulder? A possible feasible mechanism is obtained by separating the

two universal joints (Fig. 9). Indeed, the shoulder mechanism as presented in Figure 8 is not directly a possible solution because of the superimposed universal joints. The change in joint location does not alter the kinematic properties of the system. Indeed, the kinematics are still defined by a set of polynomial equations ((15)-(24)) with the difference that one of the ellipsoid equations is translated away from the origin. Also, the minimal coordinate construction method remains the same.

It is of course not necessary to impose the ellipsoid nature of the scapulothoracic gliding plane on the length of the legs $B_2 - P_2$ and $B_3 - P_3$. One could impose spherical behaviour or even planar behaviour ((31)-(32)). This would considerably simplify the description of the platforms motion. In both cases the point P_2 would be described with respect to P_3 , using a polar coordinate. For spherical behaviour, P_2 moves on the intersection of two spheres which is a circle. For planar behaviour, P_2 moves in a circle around P_3 .

$$\mathbf{P}_2 : ax + by + cz = d, \quad (31)$$

$$\mathbf{P}_3 : ax + by + cz = d. \quad (32)$$

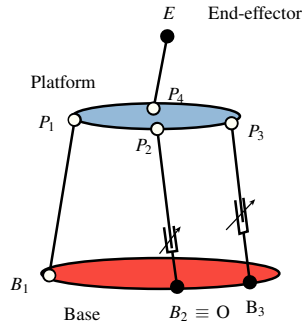


Fig. 9. Schematic of a robotic humanoid shoulder mechanism with identical kinematic characteristics to the shoulder.

Before a physical implementation of the system is considered, it would be necessary to investigate their kinematics in detail to locate any possible singular points and whether or not the control is actually possible. Additionally, the structural properties of such systems should also require attention.

B. Platform Control & Motion Planning

The minimal coordinates presented in this paper have the property of being differentially independent and can be expressed as functions of the joint coordinates. The joint coordinates can also be expressed as functions of the minimal coordinates. Therefore, they represent the flat outputs of the system of which they describe the motion [31]. Indeed, the shoulder model and the humanoid mechanism are differentially flat systems.

Flat systems are of interest because they make motion planning straightforward and allow the development of trajectory tracking control strategies. Differential flatness has been for instance, extensively used to plan the motion of a car with

n trailers [32]. Differential flatness has also been used to develop a control strategy for a crane [33].

Practically, the motion of a flat system can be obtained by planning the motion of each of the flat outputs independently using the following polynomial equation.

$$m_i(t) = m_i(t_0) + \sum_{j=1}^n p_j (m_i(T) - m_i(t_0)) \left(\frac{t-t_0}{T-t_0} \right)^j. \quad (33)$$

Combined with the coordinate map χ ((30)), an end-effector path can easily be planned and controlled.

C. Other Applications

The simplicity of motion planning using the minimal coordinates can be applied to other problems than control of a humanoid mechanism. Indeed, the scapulohumeral rhythm discussed in Section II-G could also be modelled using the minimal coordinates. The methods proposed so far use measured data, either directly ([34], [35]) or to construct regression models ([7], [16], [17]), which is difficult to obtain. Additionally, inverse kinematics, cannot easily reproduce the level of coordination exhibited by the physical system [19]. If combined with measured data, the minimal coordinates could provide a high-quality nonlinear description of the scapulohumeral rhythm.

V. CONCLUSIONS

In this paper the kinematics of the anatomical shoulder are described using a model from the biomechanics literature. The kinematic model is then compared to a 3-3 Stewart platform, thereby underlining the parallel structure of the shoulder. A new method is proposed for solving the shoulder kinematic indeterminacy, using minimal coordinates. The coordinates are constructed from simple geometric relations between bony landmarks and the scapulothoracic gliding plane constraints. A humanoid robotic shoulder mechanism is then proposed based on an identical kinematic structure as the shoulder model. It is shown how a set of minimal coordinates can easily be obtained for such a system using the same approach as the shoulder. A possible control strategy is discussed along with considerations on feasibility.

The coordinates are advantageous in the simplicity with which they can be applied. They also present an attractive solution for control strategies since they can be considered as flat outputs of the system.

APPENDIX

A. Constructing the Scapulothoracic Constraints

In the ellipsoid reference frame, the projections TSp and AIp of the points TS and AI onto the ellipsoid satisfy the ellipsoid equations (23)-(24). They can also be computed in terms of the coordinates of TS and AI. Considering the point TS, the point TSp is obtained by

$$\mathbf{TSp} = \mathbf{TS} + \eta \mathbf{n}, \quad (A.1)$$

where \mathbf{n} is the normal to the surface and η a scalar factor. The normal to the surface of the ellipsoid is defined by

$$\mathbf{n} = \left(\frac{2x}{a^2} \quad \frac{2y}{b^2} \quad \frac{2z}{c^2} \right)^T, \quad (A.2)$$

where (x, y, z) are the coordinates of the point where the normal is evaluated. Using this relation in (A.1) leads to

$$\begin{pmatrix} x & y & z \end{pmatrix}^T = \begin{pmatrix} \bar{z}_1 & \bar{z}_2 & \bar{z}_3 \end{pmatrix}^T + \eta \begin{pmatrix} \frac{2x}{a^2} & \frac{2y}{b^2} & \frac{2z}{c^2} \end{pmatrix}^T \quad (\text{A.3})$$

Finally the point TSp is defined by

$$\mathbf{TSp} = (z_1 \quad z_2 \quad z_3)^T = \begin{pmatrix} \frac{a^2 \bar{z}_1}{a^2 - 2\eta} & \frac{b^2 \bar{z}_2}{b^2 - 2\eta} & \frac{c^2 \bar{z}_3}{c^2 - 2\eta} \end{pmatrix}^T \quad (\text{A.4})$$

The constraint equation is therefore defined by

$$\Phi_{\text{TS}} = \frac{a^2 z_1^2}{(a^2 - 2\eta)^2} + \frac{b^2 z_2^2}{(b^2 - 2\eta)^2} + \frac{c^2 z_3^2}{(c^2 - 2\eta)^2} - 1 = 0 \quad (\text{A.5})$$

The parameter η remains the same if the normal vector is normalised, and can therefore be computed in the initial position using a nonlinear function solver. The second constraint is exactly identical.

B. Constructing the Sphere-Ellipsoid Intersection

The point TS is constrained by the following equations which define a locus of points.

$$z_1^2/a_1^2 + z_2^2/b_1^2 + z_3^2/c_1^2 - 1 = 0, \quad (\text{B.1})$$

$$(z_1 - u_1)^2 + (z_2 - u_2)^2 + (z_3 - u_3)^2 - \|\mathbf{P}_1 - \mathbf{P}_3\|^2 = 0. \quad (\text{B.2})$$

The two equations define the intersection between a sphere and an ellipsoid. In Section IV it is stated that the solution is described in terms of the the z coordinate of the point P_2 and the coordinates of the point P_3 . The first step towards solving the intersection problem is to define one of the coordinates as function of the others. Using the first equation leads to

$$z_1 = Z(z_2, z_3) = \pm a \sqrt{1 - z_2^2/b^2 - z_3^2/c^2}. \quad (\text{B.3})$$

This solution is then inserted into the second equation (A.2) yielding a polynomial function in z_2 where the coefficients are real functions of z_3, u_1, u_2 and u_3

$$\begin{aligned} P_4 z_2^4 + P_3 z_2^3 + P_2 z_2^2 + P_1 z_2 + P_0 &= 0, & (\text{B.4}) \\ P_i &= P_i(z_3, u_1, u_2, u_3) \quad i = 0, 1, 2, 3, 4. \end{aligned}$$

Equation (B.4) is a quartic equation in z_2 . The equation has an analytical solution s_1 given by Ferrari's method [37]. The solution to the equation yields four roots which are function of z_3, y_1, y_2 and y_3 .

$$\begin{aligned} (z_2 - s_1)(z_2 - s_2)(z_2 - s_3)(z_2 - s_4) &= 0, & (\text{B.5}) \\ s_i &= S_i(z_3, u_1, u_2, u_3), \quad i = 1, 2, 3, 4. \end{aligned}$$

Since the coefficients are all real, the roots will be a pair of real roots (s_1, s_2) and a pair of complex conjugate roots (s_3, s_4) . This will be the case as long as the coordinate z_3 remains inside a certain interval. Indeed, the z_3 coordinate cannot take any value and must remain within

$$z_3 \in [(z_3)_{\min}, (z_3)_{\max}]. \quad (\text{B.6})$$

The extremal values for z_3 are located at the point where the real roots of (B.4) are identical. In Ferrari's method, this condition leads to a nonlinear equation in z_3 which can be solved using the Newton-Raphson method. Running

the algorithm twice from initial values with opposite signs leads to the two values $(z_3)_{\min}$ and $(z_3)_{\max}$. These values are themselves functions of the point P_3 's coordinates u_1, u_2 and u_3 , which change as the point P_3 moves. Thus, the locus of points defined by the intersection of the ellipsoid and sphere are parameterised as a function of z_3 .

$$z_1 : Z(z_3, u_1, u_2, u_3) = \begin{cases} \pm a \sqrt{1 - s_1^2/b^2 - z_3^2/c^2} \\ \pm a \sqrt{1 - s_2^2/b^2 - z_3^2/c^2} \end{cases}, \quad (\text{B.7})$$

$$z_2 : S(z_3, u_1, u_2, u_3) = \begin{cases} s_1(z_3, u_1, u_2, u_3) \\ s_2(z_3, u_1, u_2, u_3) \end{cases}, \quad (\text{B.8})$$

$$z_3 : z_3 \in [(z_3)_{\min}(u_1, u_2, u_3), (z_3)_{\max}(u_1, u_2, u_3)]. \quad (\text{B.9})$$

The z_2 coordinate has four solutions, two of which are valid. The two invalid solutions are eliminated by testing if the solutions validate the sphere equation (B.2). Since the z_1 coordinate is solved using the ellipsoid equation (B.1), the solutions must also hold for the sphere equation. This is achieved by testing the following equality

$$\begin{aligned} (Z(z_3, s_i) - u_1)^2 + (s_i - u_2)^2 + (z_3 - u_3)^2 &= \dots \\ - \|\mathbf{P}_2 - \mathbf{P}_3\|^2, \quad i = 1, 2. & \quad (\text{B.10}) \end{aligned}$$

This test eliminates two of the four solutions from (B.7). Figure 10 illustrates an example of the locus of points obtained from the intersection of a sphere and ellipsoid.

Lastly, the coordinate z_3 can be replaced by the relative coordinate μ defined below. This will make its planning easier.

$$z_3 = (z_3)_{\min} + \mu \cdot ((z_3)_{\max} - (z_3)_{\min}), \quad \mu \in [0, 1]. \quad (\text{B.11})$$

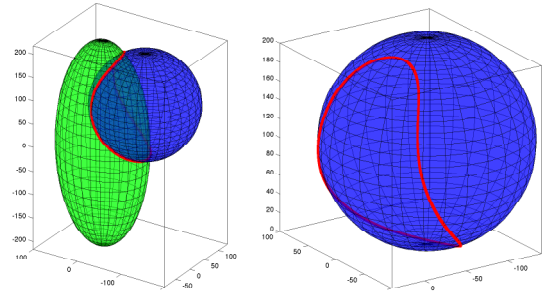


Fig. 10. Example of the ellipsoid-sphere intersection locus (in red).

ACKNOWLEDGMENT

This study was supported by the Swiss National Science Foundation (K-32K1 122512).

REFERENCES

- [1] W. T. Dempster, Mechanism of shoulder movement, Archives of Physical Medicine and Rehabilitation, vol. 46, no. 1, pp. 49 - 69, 1965.
- [2] A. E. Engin and S. M. Chen, Statistical data base for the biomechanical properties of the human shoulder complex - part i : Kinematics of the shoulder complex, Journal of biomechanical engineering, vol. 108, pp. 215 - 221, 1986.
- [3] A. E. Engin and S. M. Chen, Statistical data base for the biomechanical properties of the human shoulder complex - part ii : Passive resistive properties beyond the shoulder complex sinus, Journal of biomechanical engineering, vol. 108, pp. 222 - 227, 1986.

- [4] A. E. Engin and S. T. Tumer, Three-dimensional kinematic modelling of the human shoulder complex - part i: Physical model and determination of joint sinus cones, *Journal of biomechanical engineering*, vol. 111, no. 2, pp. 107 - 112, 1989.
- [5] A. E. Engin and S. T. Tumer, Three-dimensional kinematic modeling of the human shoulder complex - part ii: Mathematical modeling and solution via optimization, *Journal of biomechanical engineering*, vol. 111, no. 2, pp. 113 - 221, 1989.
- [6] C. Hogfors, B. Peterson, and P. Herberts, Biomechanical model of the human shoulder-i. elements, *Journal of biomechanics*, vol. 20, no. 2, pp. 157 - 166, 1987.
- [7] C. Hogfors, B. Peterson, G. Sigholm, and P. Herberts, Biomechanical model of the human shoulder-ii. the shoulder rythm, *Journal of biomechanics*, vol. 24, no. 8, pp. 699 - 709, 1991.
- [8] F. C. T. van der Helm, A finite element musculoskeletal model of the shoulder mechanism, *Journal of Biomechanics*, vol. 27, no. 5, pp. 551 - 553, 555 - 569, 1994.
- [9] G. Wu, F. C. T. van der Helm, H. Veeger, M. Makhsous, P. Van Roy, C. Anglin, J. Nagels, A. Karduna, K. McQuade, X. Wang, F. Werner, and B. Buchholz, ISB recommendation on definitions of joint coordinate systems of various joints for the reporting of human joint motion - part ii: shoulder, elbow, wrist and hand, *Journal of Biomechanics*, vol. 38, no. 5, pp. 981 - 992, 2005.
- [10] M. Rosheim, In the footsteps of leonardo [articulated anthropomorphic robot], *Robotics Automation Magazine, IEEE*, vol. 4, no. 2, pp. 12 - 14, 1997.
- [11] M. Okada and Y. Nakamura, Development of a cybernetic shoulder-a 3-dof mechanism that imitates biological shoulder motion, *Robotics, IEEE Transactions on*, vol. 21, no. 3, pp. 438 - 444, 1999.
- [12] J. Lenarcic and M. Stanisic, A humanoid shoulder complex and the humeral pointing kinematics, *Robotics and Automation, IEEE Transactions on*, vol. 19, no. 3, pp. 499 - 506, june 2003.
- [13] M. M. Stanisic, J. M. Witala, and J. T. Feix, A dexterous humanoid shoulder mechanism, *Journal of Robotic Systems*, vol. 18, no. 12, pp. 737 - 745, 2001.
- [14] Y. Sodeyama, I. Mizuuchi, T. Yoshikai, Y. Nakanishi, and M. Inaba, A shoulder structure of muscle-driven humanoid with shoulder blades, in *Intelligent Robots and Systems. (IROS 2005). 2005 IEEE/RSJ International Conference on*, pp. 4028 - 4033, 2005.
- [15] S. Ikemoto, F. Kannou, and K. Hosoda, Humanlike shoulder complex for musculoskeletal robot arms, in *Intelligent Robots and Systems (IROS), 2012 IEEE/RSJ International Conference on*, pp. 4892 - 4897, 2012.
- [16] J. H. deGroot and R. Brand, A three-dimension regression model of the shoulder rhythm, *Clinical biomechanics*, vol. 16, pp. 735 - 743, 2001.
- [17] T.-J. Grewal, Quantifying the shoulder rhythm and comparing non-invasive methods of scapular tracking for overhead and axially rotated humeral postures, Ph.D. dissertation, University of Waterloo, Waterloo, 2011.
- [18] O. Khatib, E. Demircan, V. De Sapio, L. Sentis, T. Besier, and S. Delp, Robotics-based synthesis of human motion, *Journal of Physiology*, vol. 103, pp. 211 - 219, 2009.
- [19] W. Maurel, 3d modeling of the human upper limb including the biomechanics of joints, muscles and soft tissues, Ph.D. dissertation, EPFL, Lausanne, 1998.
- [20] B. Garner and M. Pandy, Musculoskeletal model of the upper limb based on the visible human male dataset, *Computer Methods in Biomechanics and Biomedical Engineering*, vol. 4, no. 2, pp. 107 - 124, 1999.
- [21] J. Burdick, Kinematic analysis and design of redundant robot manipulators, Ph.D. dissertation, Stanford, Stanford, 1988.
- [22] X. Wang, M. Maurin, F. Mazet, N. De Castro Maia, K. Voinot, J. Verriest, and M. Fayet, Three-dimensional modelling of the motion range of axial rotation of the upper arm, *Journal of Biomechanics*, vol. 31, no. 10, pp. 899 - 908, 1998.
- [23] L. Herda, R. Urtasun, and A. Hanson, Automatic determination of shoulder joint limits using quaternion field boundaries, In *Proceedings of the 5th International Conference on Automatic Face and Gesture Recognition*, vol. 2002, pp. 95 - 100, 2002.
- [24] E. Conkur and R. Buckingham, Clarifying the definition of redundancy as used in robotics, *Robotica*, vol. 15, p. 583 - 586, 1997.
- [25] R. Cailliet, *The Illustrated Guide to Functional Anatomy of the Musculoskeletal System*. American Medical Association, 2004.
- [26] L. Freedman and R. Munro, Abduction of the arm in the scapular plane: Scapular and glenohumeral movements a roentgenographic study, *The Journal of Bone & Joint Surgery*, vol. 48, no. 8, pp. 1503 - 1510, 1966.
- [27] I. Michiels and J. Grevenstein, Kinematics of shoulder abduction in the scapular plane: On the influence of abduction velocity and external load, *Clinical Biomechanics*, vol. 10, no. 3, pp. 137 - 143, 1995.
- [28] B. Dasgupta and T. Mruthyunjaya, The Stewart platform manipulator: a review, *Mechanism and Machine Theory*, vol. 35, no. 1, pp. 15 - 40, 2000.
- [29] B. Buchberger, Groebner bases and systems theory, *Multidimensional Syst. Signal Process.*, vol. 12, no. 3-4, pp. 223 - 251, Jul. 2001.
- [30] Cox D., Little J., O'Shea D., "Ideals, Varieties, and Algorithms," New-York, Springer, 2007.
- [31] J. Levine, On necessary and sufficient conditions for differential flatness, *Appl. Algebra Eng., Commun. Comput.*, vol. 22, no. 1, pp. 47 - 90, Jan. 2011.
- [32] P. Rouchon, M. Fliess, J. Levine, and P. Martin, Flatness, motion planning and trailer systems, in *Decision and Control, 1993., Proceedings of the 32nd IEEE Conference on*, vol. 3, pp. 2700 - 2705, dec 1993.
- [33] D. Bucciari, C. Salzmann, P. Mullhaupt, and D. Bonvin, Jet-scheduling control for spidercrane: Experimental results, in *17th IFAC World Congress (IFAC08)*, 2008.
- [34] R. Happee, Inverse dynamic optimization including muscular dynamics, a new simulation method applied to goal directed movements, *Journal of Biomechanics*, vol. 27, no. 7, pp. 953 - 960, 1994.
- [35] C. Quental, J. Folgado, J. Ambrósio, and J. Monteiro, A multibody biomechanical model of the upper limb including the shoulder girdle, *Multibody System Dynamics*, vol. 28, pp. 83 - 108, 2012.
- [36] V. De Sapio, K. Holzbaaur, and O. Khatib, The control of kinematically constrained shoulder complexes: physiological and humanoid examples, in *Robotics and Automation, 2006. ICRA 2006. Proceedings 2006 IEEE International Conference on*, pp. 2952 - 2959, 2006.
- [37] G. Cardano, *Ars magna or The Rules of Algebra*. Dover (published 1993), 1545.